Temperature-Induced Inactivation of Cytoplasmic Biogel Osmosensing Properties is Associated with Suppression of Regulatory Volume Decrease in A549 Cells

Alexandra Platonova · Francis Boudreault · Leonid V. Kapilevich ·
Georgy V. Maksimov · Olga Ponomarchuk · Ryszard Grygorczyk ·
Sergei N. Orlov

Abstract Upstream intermediates of intracellular signaling involved in cell volume regulation remain poorly explored. Recently, we demonstrated that osmolarity-induced volume changes in permeabilized cells were several-fold higher than those observed with intact cells, indicating the osmosensing properties of cytoplasmic gel. To further examine the role of cytoplasmic biogel in cell volume regulation, we compared the action of short-term heat treatment on volume changes in intact and permeabilized A549 cells. Pretreatment of A549 cells at 48 °C suppressed swelling triggered by dissipation of Donnan's equilibrium as well as by hyposmotic medium. Significantly, heat treatment completely abolished the action of hyposomotic medium on volume changes in permeabilized cells, showing that temperature elevation suppresses osmosensing properties via its effect on biogel rather than on plasma membrane water permeability. Identical heat treatment blocked the regulatory volume decrease (RVD) as well as the increment of Ba^{2+}-sensitive K^+-channel activity seen in control cells exposed to hyposmotic swelling. Unlike swelling, hyperosmotic shrinkage was decreased by twofold in cells subjected to 10-min preincubation at 50 °C. Our results disclose that osmosensing by cytoplasmic gel is a key event in the RVD triggered by hypotonic swelling. The role of biogel and plasma membrane in intracellular signaling triggered by hyperosmotic shrinkage should be further investigated.

Keywords Cell volume · Permeabilized A549 cells · Cytoplasmic biogel · Regulatory volume decrease · K^+ fluxes

A. Platonova · F. Boudreault · O. Ponomarchuk ·
R. Grygorczyk · S. N. Orlov
Research Centre, Centre hospitalier de l' Université de Montréal (CRCHUM), Montreal, QC, Canada

L. V. Kapilevich · S. N. Orlov
Tomsk State University, Tomsk, Russia

G. V. Maksimov · O. Ponomarchuk · S. N. Orlov (✉)
Laboratory of Biological Membranes, Faculty of Biology, M.V. Lomonosov Moscow State University, Vorob'evy Gory 1/12, Moscow 119899, Russia
e-mail: sergeinorlov@yandex.ru

R. Grygorczyk · S. N. Orlov
Department of Medicine, Faculty of Medicine, University of Montreal, Montreal, QC, Canada

Introduction

Changes in cell volume occur frequently under physiological and pathological conditions due to alterations in extra- or intracellular osmolyte concentrations. When they arise, such changes impact a plethora of cellular functions, including macromolecular synthesis and catabolism, cell proliferation, differentiation, and death (Lang et al. 1998; Hoffmann et al. 2009; Orlov et al. 2013). Thus, cells regulate their volume with an accuracy of ∼99 % (Kuang et al. 2006) via accumulation or loss of intracellular osmolytes. The resulting compensatory processes are termed regulatory volume increase (RVI) and regulatory volume decrease (RVD) (for comprehensive reviews, refer to Lang et al. 1998; Mongin and Orlov 2001; O'Neill 1999; Hoffmann and Simonsen 1989).

Despite numerous efforts, the molecular origin of cell volume sensors and upstream signaling events that lead to RVI and RVD activation remains poorly understood. Thus, it has been proposed that the plasma membranes

of swollen cells are stretched, leading, in turn, to conformational changes in the mechano-sensitive bacterial channels MscL and MscS (Martinac 2011) as well as members of the transient receptor potential vanilloid subfamily (O'Neil and Heller 2005; Pedersen and Nilius 2007) involved in osmolyte movements providing RVD. To explore this hypothesis, Groulx and co-workers employed the dual-image surface reconstruction (DI-SUR) technique, for simultaneous measurement of cell surface area and volume with temporal resolution of ~ 100 ms. This study demonstrated that nucleated mammalian cells accommodate twofold volume which increases in the absence of plasma membrane stretch due to shape changes and membrane unfolding (Groulx et al. 2006).

In 1903, Nickolai Koltsov proposed that the architecture of nucleated cells is supported by a intracellular cytoskeleton (http://en.wikipedia.org/wiki/Cytoskeleton). Later on, several research groups presented evidence of possible involvement of this three-dimensional (3D) structure formed by actin microfilaments, microtubules, and intermediate filaments in cell volume sensing. Indeed, actin microfilaments have been found to be depolymerized and polymerized in a variety of non-adherent swollen and shrunken cells, respectively. Moreover, in several cell types, the addition of F-actin-disrupting agents (cytochalasins) and microtubule depolymerization agents (colchicine) suppressed RVI/RVD and other volume-sensitive cellular responses (for review, refer to Papakonstanti et al. 2000; Di Ciano-Oliveira et al. 2006; Jakab et al. 2002; Hoffmann et al. 2009). It should be noted, however, that negative results were obtained in a study on the actions of these compounds on RVD in human neutrophils (Downey et al. 1995), HL-60 (Downey et al. 1995; Hallows et al. 1991, 1996) and A549 cells (Platonova et al. 2013). Moreover, in bovine articular chondrocytes, depolymerization of the actin cytoskeleton accelerated rather than suppressed post-RVD RVI (Kerrigan et al. 2006).

In the 1980s and early 1990s, several research groups proposed that intramolecular interactions stemming from high concentrations of macromolecules in the cytoplasm (so-called macromolecular crowding) crucially affect molecular and cellular functions (Minton 1981; Fulton 1982). These data, and the notion that even small changes in intracellular water content affect macromolecular crowding, prompted researchers to propose that alterations in macromolecular crowding may serve as cell volume sensors (Minton et al. 1992; Parker 1993). Indeed, in dog erythrocytes, shrinkage-activated Na^+/H^+ exchange and swelling-activated K^+, Cl^- cotransport were observed when hemoglobin content within resealed ghosts exceeded 300 mg/ml, corresponding to its value

in intact cells. Significantly, the activation set points of both carriers were affected by modulation of intracellular macromolecular crowding rather than cell volume per se (Colclasure and Parker 1992; Parker 1993). However, in contrast to dog red blood cells, volume elevation of resealed human erythrocyte ghosts activated K^+, Cl^- cotransport, even though solute concentration was constant, and ghosts were virtually free of proteins (Sachs 1998). Summers et al. (1997) examined the volume of internally perfused barnacle muscle cells under constant ionic strength, osmolality, and membrane stretch. They observed that cell volume attenuation by reduction of intracellular content of ovalbumin or a polymer with molecular weight of ~ 20 kDa was abolished by RVD inhibitors. To the best of our knowledge, this paper, published 15 years ago, remains the only evidence implicating macromolecular crowding in volume regulation of nucleated cells.

Because of macromolecular crowding and cytoskeleton network-mediated compartmentalization, the cytoplasm exists as an aqueous biogel (Luby-Phelps 2000). This conclusion was initially supported by data showing that squid axoplasm retains its cylindrical shape after extrusion from giant axons into high-K^+ solution (Brown and Lasek 1993). Recently, we demonstrated that plasma membrane permeabilization with modest concentrations of digitonin or amphotericin B leads to dissipation of Donnan's equilibrium and cell swelling, but does not affect the integrity of nucleated mammalian cells (Fels et al. 2009). Unexpectedly, we found that permeabilized cells swell and shrink in hypo- and hypertonic solutions, respectively. Moreover, osmolarity-induced volume changes were several-fold larger than those observed with intact cells, consistent with the cytoplasm's high water-binding capacity. Because binding or release of large amounts of water may allow rapid modulation of local fluidity, macromolecular crowding, and activity of the intracellular environment, these findings suggest that cytoplasmic hydrogel functions as an osmosensor. In this study, we also noted that a van't Hoff relationship between volume and inverse osmolality exhibits 3.7-fold steeper dependence in permeabilized cells as compared to intact counterparts. This observation demonstrates that cytoplasmic gel behaves like a highly sensitive linear osmometer and suggests that the stable steady-state volume is maintained by the plasma membrane, which prevents uncontrolled leakage of osmolytes and reduces intracellular osmotic pressure by energy-dependent ion pumping.

It was shown that brief exposure of mammalian erythrocytes at 49–50 °C completely abolished the regulation of Na^+, K^+, $2Cl^-$ cotransport, K^+, Cl^- cotransport, and Na^+/H^+ exchange triggered by cell volume perturbations (Orlov

et al. [1993](#); Parshina et al. [2013](#)). Keeping these data in mind, we explored the osmosensing properties of cytoplasm by comparing temperature dependencies of volume changes and ion fluxes triggered by anisosmotic media.

Methods

Cell culture Human lung carcinoma A549 cells were grown in Dullbecco's modified Eagle's medium supplemented with 10 % fetal bovine serum, 2 mM L-glutamine, 50 U/ml penicillin, and 100 µg/ml streptomycin, as described previously (Tatur et al. [2007](#)).

Cell volume was measured in substrate-attached cells with an improved version of the DISUR technique (Boudreault and Grygorczyk [2004](#)). The method involves 3D reconstruction of cell shape based on 2 conventional microscopy cell images acquired in 2 perpendicular directions. Side-view and top-view cell images were captured by 2 independent, miniature, charge-coupled cameras (Moticam 350, Motic Instruments Inc., Richmond, BC, Canada) with Motic software at 10- to 60-s intervals to closely follow rapid volume changes. The images served to generate a set of topographical curves of the cell surface from its digitized side-view profile and base outline. Cell volume was calculated from the reconstructed cell topographical model with MATLAB (Math Works, Inc., Natick, MA, USA). Although DISUR provides absolute cell volume values, data plots in the present study show relative volume normalized to initial intact cell volume in physiological solution. Cells seeded on coverslips were mounted in a custom-made, flow-through imaging chamber, and perfused at the rate of 1–2 ml/min with 2-[4-(2-hydroxyethyl)piperazin-1-yl]ethanesulfonic acid (HEPES)-buffered isotonic medium B (B-iso) at 37 °C. Medium B-iso was composed of 135 mM NaCl, 5 mM KCl, 1.2 mM MgSO$_4$, 1.3 mM CaCl$_2$, 1.2 mM Na$_2$HPO$_4$, 10 mM D-glucose, 10 mM HEPES, pH 7.4, adjusted with NaOH. In hyposmotic medium B (B-hypo), NaCl was decreased to 70 mM. Hyperosmotic medium B (B-hyper) contained 200 mM mannitol.

Intracellular water volume in cells seeded in 12-well plates was measured as [^{14}C]-urea available space according to a previously described protocol (Orlov et al. [1996](#)) and calculated as $V = A_c/A_m m$, where A_c was the radioactivity of the cells after 30-min incubation with 2 Ci/ml [^{14}C]-urea (dpm), A_m was the radioactivity of the incubation medium (dmp/l), and m was protein content in the cell lysate (mg).

Plasma membranes were permeabilized by ~2-min exposure to 5 µg/ml (~4 µM) of digitonin (Sigma-Aldrich) in intracellular-like solution (ILS) containing 10 mM NaCl, 110 mM KCl, 5 mM MgCl$_2$, 1 mM Na-

ATP, 1 mM EGTA, 11 mM dithiothreitol, 25 mM imidazole, and 10 mM 2-[[1,3-dihydroxy-2-(hydroxymethyl)propan-2-yl]amino]ethanesulfonic acid (pH 7.1), followed by washing with digitonin-free ILS. In some experiments, ILS osmolality was reduced by decreasing KCl concentration to 70 mM (ILS-hypo). As verified by trypan blue staining, ~90 % of A549 cells were permeabilized by such treatment. In separate experiments, adding trypan blue at different time points after digitonin treatment revealed that ~70 % of cells remained permeabilized for at least 30 min, long enough to study the properties of such permeabilized cells. Because some cells resealed their plasma membrane during the 30–40-min period, trypan blue staining was always undertaken at the end of each experiment, to verify that the plasma membrane of any given cell under study remained permeabilized throughout. Cells that failed this test were rejected from analysis.

^{86}Rb *uptake* was measured in cells growing in 24-well plates, washed twice with 2 ml of medium containing 150 mM NaCl, 1 mM MgCl$_2$, 1 mM CaCl$_2$, and 10 mM HEPES–tris buffer (pH 7.4, room temperature) and incubated for 30 min at 37 °C in 1 ml of B-iso medium. The preincubation medium was then replaced by 0.5 ml of medium containing 0.5–1 µCi/ml ^{86}RbCl, 10 µM ouabain, 10 µM bumetanide, or 1 mM BaCl$_2$. The osmolality of this medium was varied by adding mannitol or by reducing NaCl concentration. Preliminary experiments demonstrated that, in these media, ^{86}Rb uptake was linear up-to 20 min. This considered isotope uptake was terminated in 10 min by adding 2 ml of ice-cold medium containing 100 mM MgCl$_2$ and 10 mM HEPES–tris buffer (pH 7.4). The cells were then transferred on ice, washed 4 times with 2 ml of the same ice-cold medium, and lysed with 1 ml of 1 % SDS/4 mM EDTA mixture. Radioactivity of the cell lysate was measured with a liquid scintillation analyzer, and ion uptake was calculated as $V = A/amt,$ where A was radioactivity in the sample (cpm), a was the specific radioactivity of ^{86}Rb (K$^+$) in the incubation medium, m was protein content in the sample (mg), and t was incubation time (min). Na$^+$, K$^+$, 2Cl$^-$ cotransport activity was quantified as the ouabain-resistant, bumetanide-sensitive component of the ^{86}Rb influx rate. Previously, we reported that, side-by-side with K$^+$ channels, Ba^{2+} dose-dependently inhibited Na$^+$, K$^+$, 2Cl$^-$ cotransport (Gagnon et al. [1999](#)). With these data in mind, the activity of K$^+$ channels was estimated as (ouabain + bumetanide)-resistant, Ba^{2+}-sensitive ^{86}Rb influx.

Intracellular content of exchangeable sodium, potassium, and chloride was determined as steady-state distribution of ^{22}Na, ^{86}Rb, and ^{36}Cl. To establish isotope equilibrium, cells growing in 12-well plates were preincubated for 3 h in medium B containing 0.5 Ci/ml ^{86}RbCl, 4 Ci/ml ^{22}NaCl, or 3 Ci/ml H^{36}Cl and washed 4 times with
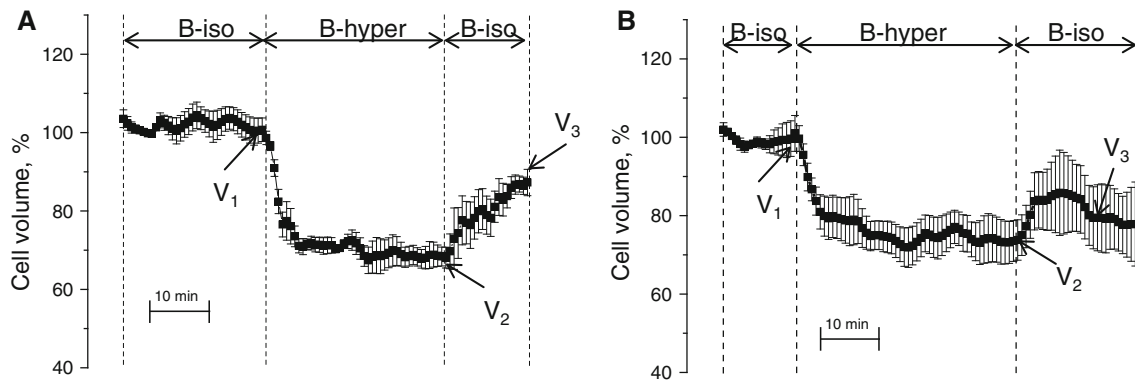
Fig. 1 Effect of hyperosmotic medium (B-hyper) on volume changes in control A549 cells (**a**) and A549 cells subjected to 10-min preincubation at 48 °C (**b**). Note that cell volume was measured at 37 °C. Mean ± SE from 4 independent experiments are reported. Mean cell volume value documented during the first 5 min of incubation was considered as 100 %
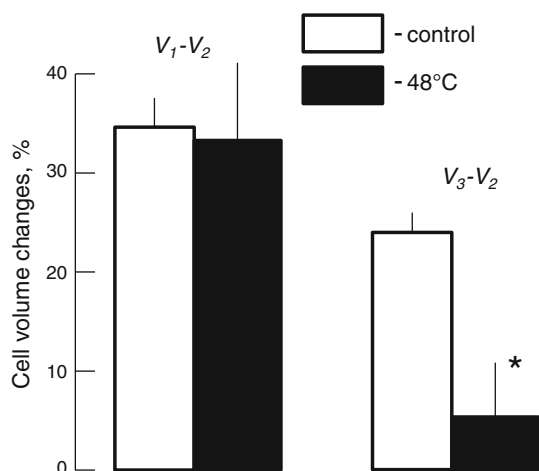

Fig. 2 Effect of 10-min preincubation at 48 °C on hyperosmotic shrinkage (parameter $V_1 - V_2$) and volume recovery in isosmotic medium (parameter $V_3 - V_2$). For time points selected for V_1, V_2, and V_3 measurements, see Fig. 1a. Note that cell volume was measured at 37 °C. Mean ± SE from 4 independent experiments are reported. *$p < 0.02$ compared to the controls

2 ml of ice-cold phosphate-buffered saline. The washing medium was aspirated and the cells lysed with 1 % SDS and 4 mM EDTA solution. Radioactivity of the incubation media and cell lysates was quantified, and intracellular cation content was calculated as A/am, where A was the radioactivity of the samples (cpm), a was the specific radioactivity of ^{86}Rb (K$^+$), ^{22}Na, or ^{36}Cl in medium (cpm/nmol), and m was protein content (mg). For more details, see (Akimova et al. 2005). Intracellular Na$^+$, K$^+$, and Cl$^-$ concentrations were calculated on the basis of intracellular water volume measurement.

Chemicals were procured from Gibco BRL (Gaithersburg, MO, USA), Calbiochem (La Jolla, CA, USA), Sigma (St. Louis, MO, USA), and Anachemia (Montreal, QC). ^{22}NaCl, ^{86}RbCl, H^{36}Cl, and [^{14}C]-urea were obtained from PerkinElmer (Waltham, MA, USA) and Isotope (St. Petersburg, Russia).

Results

Medium osmolality elevation by ~ 400 mOsm, triggered by the addition of 200 mM mannitol to isosmotic medium B, resulted in attenuation of cell volume by ~ 35 % (Fig. 1a). Consistent with previous observations (Fels et al. 2009), we did not detect any significant RVI during the next 30-min incubation of A549 cells. Transfer of cells to a isosmotic environment culminated in slow cell volume restoration that was not completed within 15 min. 10-min preincubation of A549 cells at 48 °C did not significantly affect the kinetics of hyperosmotic shrinkage measured at 37 °C (Fig. 1b), but suppressed cell volume recovery in isosmotic medium (Fig. 2, parameter $V_3 - V_2$). We also noted that the recovery slopes starting at V_2 were greater in heat-treated compared to control cells. However, because of the large values of standard errors in experiments with heat-treated cells (Fig. 1b), these differences were not statistically significant.

In contrast to sustained hyperosmotic shrinkage, hypotonic swelling of A549 cells, developing in the first 5 min of their exposure to hypotonic solution, evoked almost complete normalization of their volume in 30 min of incubation (Fig. 3a). As detected in a large number of cell types studied so far (Lang et al. 1998; Hoffmann et al. 2009), reperfusion of hypotonically treated A549 cells in isosmotic medium elicited rapid attenuation of cell volume by 30–40 % (so-called post-RVD/RVI protocol). Figure 3a displays that RVD in hyposmotically swollen cells composed of rapid and delayed components. Figures 3b and 4 show that 10-min preincubation at 48 °C almost completely abolished hyposmotic swelling of A549 cells
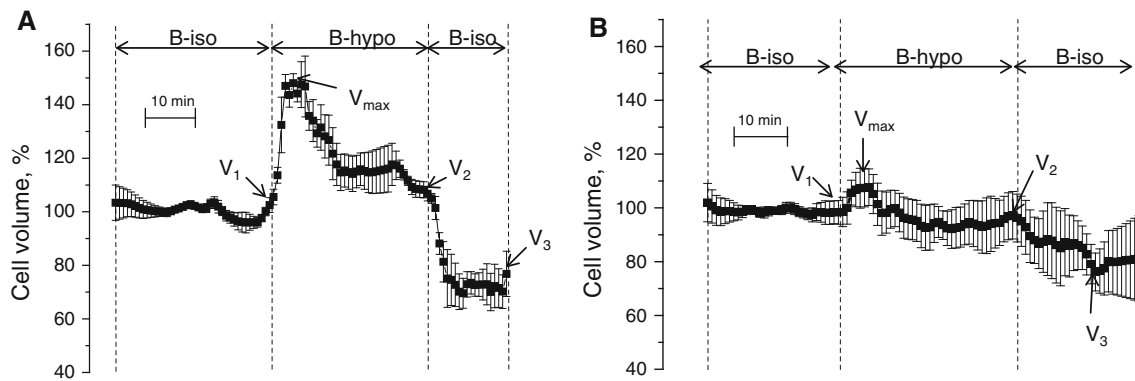
Fig. 3 Effect of hyposmotic medium (B-hypo) on volume changes in control A549 cells (**a**) and A549 cells subjected to 10-min preincubation at 48 °C (**b**). Note that cell volume was measured at 37 °C.

Mean ± SE from 4 independent experiments are reported. Mean cell volume value documented during the first 5 min of incubation was taken as 100 %
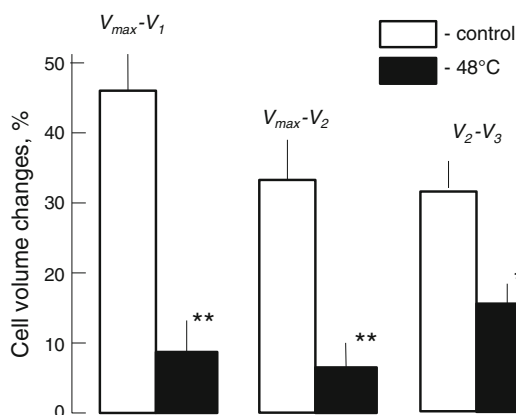

Fig. 4 Effect of 10-min preincubation at 48 °C on hyposmotic swelling (parameter $V_{max} - V_1$), RVD (parameter $V_{max} - V_2$), and isosmotic shrinkage (parameter $V_3 - V_2$). For time points selected for V_1, V_{max}, V_2, and V_3 measurements, see Fig. 3a. Note that cell volume was measured at 37 °C. Mean ± SE from 4 independent experiments are reported. *$p < 0.02$ and **$p < 0.001$ compared to the controls

(parameter $V_{max} - V_1$) as well as RVD (parameter $V_{max} - V_2$). The negligible shrinkage triggered by transfer of heat-treated cells from hyposmotic to isosmotic medium (Fig. 4, parameter $V_2 - V_3$) is consistent with the lack of their volume modulation in hyposmotic medium (parameter $V_{max} - V_1$).

Figure 5a illustrates that cell transfer in low-Na$^+$, high-K$^+$ ILS, and subsequent plasma membrane permeabilization by the addition of digitonin led to elevation of A549 cell volume by ~ 60 % (Fig. 6, parameter $V_3 - V_1$). Cell swelling in ILS was probably caused by membrane depolarization predicted from the comparison of monovalent ion concentrations in ILS ([K$^+$]=110 ± 14 mM, [Na$^+$]=12 ± 4 mM, and [Cl$^-$]=134 ± 18 mM) and in their initial concentrations in intact cells ([K$^+$]$_i$, [Na$^+$]$_i$, and [Cl$^-$]$_i$ 120, 8, and 45 mM, respectively) that,

in turn, resulted in accumulation of chloride and dissipation of Donnan's equilibrium. Consistent with previous reports (Fels et al. 2009; Koltsova et al. 2011), A549 cell permeabilization increased rather than decreased the amplitude of hyposmotic swelling (Fig. 6, parameter $V_{max} - V_3$). As predicted, plasma membrane permeabilization by digitonin in ILS completely abolished RVI mediated by efflux of intracellular inorganic osmolytes due to dissipation of the electrochemical gradients created by plasma membrane Na$^+$, K$^+$-ATPase (Lang et al. 1998; Hoffmann et al. 2009). Cell transfer to the isosmotic environment resulted in permeabilized cell volume restoration (Fig. 6, parameter $V_{max} - V_4$). Both isosmotic swelling, triggered by dissipation of Donnan's equilibrium, and swelling in hyposmotic ILS were completely eliminated in permeabilized cells subjected to 10-min preincubation at 48 °C (Fig. 5b).

To further explore the relative contribution of transmembrane gradient of monovalent cations and biogel in cell volume changes triggered by hyposmotic medium, we compared the volume of intracellular water in control and heat-treated A549 cells. Using this approach, we observed that the volume of intracellular water measured as [^{14}C]-urea available space was increased by ~ 50 % after dissipation of transmembrane gradient of Na$^+$ and K$^+$ in ILS (Fig. 7a). Five min of cell perfusion with hypotonic high-Na$^+$, low-K$^+$ medium B led to elevation of intracellular water volume by ~ 50 % that was completely normalized during the next 25 min of incubation. In contrast, the volume of intracellular water in A549 cells treated with hypotonic high-K$^+$, low-Na$^+$ medium was increased up-to 30 min of incubation. This observation confirms data obtained by DISUR technique and suggests a key role in RVD of K$^+$ efflux along its electrochemical gradient. Consistently with DISUR data (Fig. 5), intracellular water volume changes triggered by hyposmotic medium B and
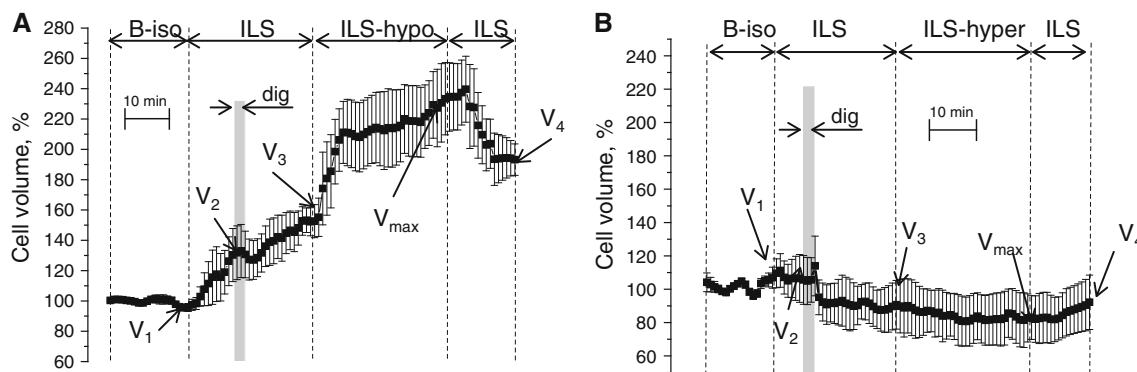
Fig. 5 Effect of hyposmotic medium (ILS-hypo) on volume changes in permeabilized control A549 cells (**a**) and permeabilized A549 cells subjected to 10-min preincubation at 48 °C (**b**). Note that cell volume

was measured at 37 °C. Mean ± SE from 4 independent experiments are reported. Mean cell volume value documented during the first 5 min of incubation was considered as 100 %
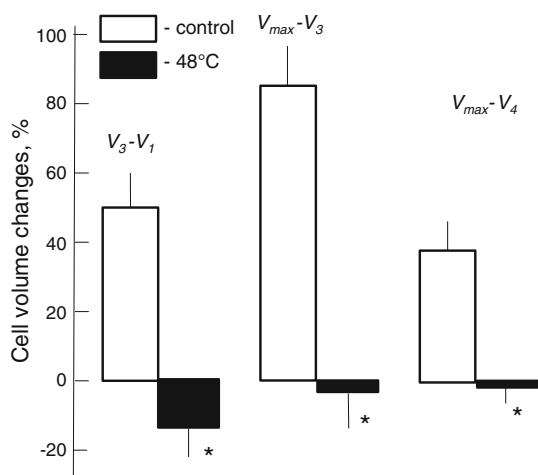

Fig. 6 Effect of 10-min preincubation at 48 °C on isosmotic swelling triggered by dissipation of Donnan's equilibrium (parameter $V_3 - V_1$), hyposmotic swelling (parameter $V_{max} - V_3$), and isosmotic shrinkage (parameter $V_{max} - V_4$) in permeabilized A549 cells. For time points selected for V_1, V_{max}, V_3, and V_4 measurements, see Fig. 5a. Note that cell volume was measured at 37 °C. Mean ± SE from 4 independent experiments are reported. *$p < 0.001$ compared to the controls

ILS were abolished by 10 min preincubation of A549 cells at 48 °C (Fig. 7b).

In subsequent experiments, we investigated the dependence of maximal amplitude of hyperosmotic shrinkage (parameter $V_2 - V_1$, Fig. 1) and hyposmotic swelling (parameter $V_{max} - V_1$, Fig. 3) on preincubation medium temperature. 10-min exposure of A549 cells at 46 °C did not change maximal hypotonic swelling amplitude, whereas temperature elevation to 48 °C decreased this parameter by 5- to 6-fold (Fig. 8, curve 1). Unlike swelling, we did not observe any significant impact of preincubation at 48 °C on cell shrinkage triggered by hyperosmotic medium. Temperature elevation to 50 °C decreased the maximal

amplitude of hyperosmotic shrinkage by twofold (Fig. 8, curve 2).

It has been shown that rapid RVI is mediated by activation of inwardly directed Na^+/H^+ exchange and Na^+, K^+, $2Cl^-$ cotransport, whereas K^+, Cl^- cotransport, and/or K^+ and Cl^- channels provide RVD via efflux of inorganic osmolytes (Lang et al. 1998; Hoffmann et al. 2009). Figure 9 illustrates that, in A549 cells, elevation of medium osmolality increases Na^+, K^+, $2Cl^-$ cotransport activity by fivefold, measured as the bumetanide-sensitive component of ^{86}Rb uptake, whereas exposure to hyposmotic medium sharply activates K^+ channels, estimated by assessment of the furosemide-resistant, Ba^{2+}-sensitive component of the ^{86}Rb influx rate. Considering these results, we investigated the dependence of Na^+, K^+, $2Cl^-$ cotransport, and K^+ channel activities on preincubation medium temperature. We noted that the baseline activities of Na^+, K^+, $2Cl^-$ cotransport, and K^+ channels, measured in isosmotic medium, were not significantly affected by elevation of preincubation medium temperature to 50 °C (Fig. 10). Increment of K^+ ($^{86}Rb^+$) influx via K^+ channels, evoked by hyposmotic swelling, was almost completely abolished by increasing preincubation medium temperature from 47 to 48 °C (Fig. 10a). In contrast, inactivation of shrinkage-sensitive Na^+, K^+, $2Cl^-$ cotransport was observed under temperature elevation in the range from 48 to 50 °C (Fig. 10b). These data are consistent with early results on temperature-induced inactivation of volume-sensitive Na^+, K^+, $2Cl^-$ cotransport in rat erythrocytes (Orlov et al. 1993).

Discussion

Previously, we demonstrated that cell volume changes triggered by anisosmotic media are preserved in permeabilized cells, indicating that cytoplasmic gel (or so-
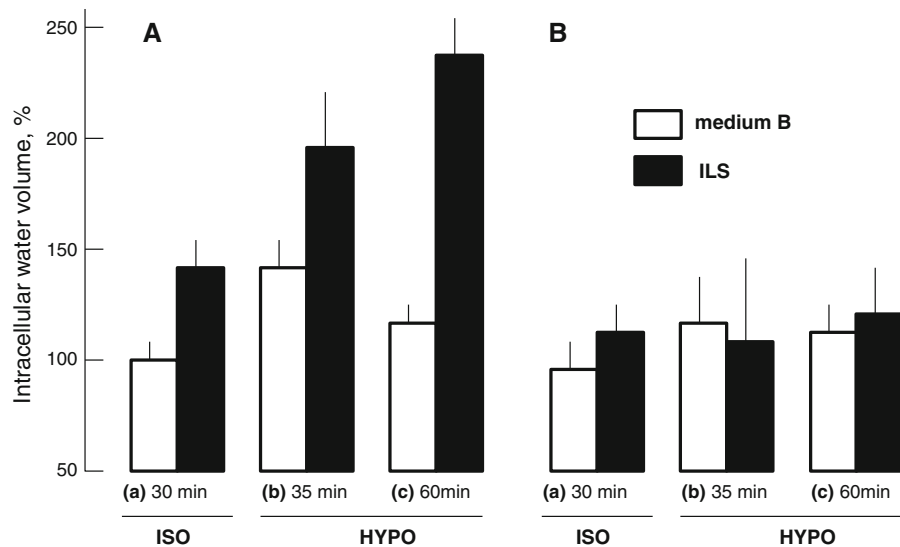
Fig. 7 Effect of hyposmotic medium on intracellular water volume in A549 cells. **a** Control cells; **b** Cells subjected to 10 min preincubation at 48 °C. Cells were perfused during 30 min with isosmotic high-Na^+, low-K^+ medium B, or high-K^+, low-Na^+ ILS, and then osmolality of these media was decreased for the next 30 min as indicated in "Methods" section. At indicated time points, the volume of intracellular water was measured as [^{14}C]-urea available space. The volume of intracellular water in control cells after 30 min incubation in medium B (1.96 ± 0.21 l/mg protein) was taken as 100 %. Mean $\pm$ SE from experiments performed in quadruplicates are shown
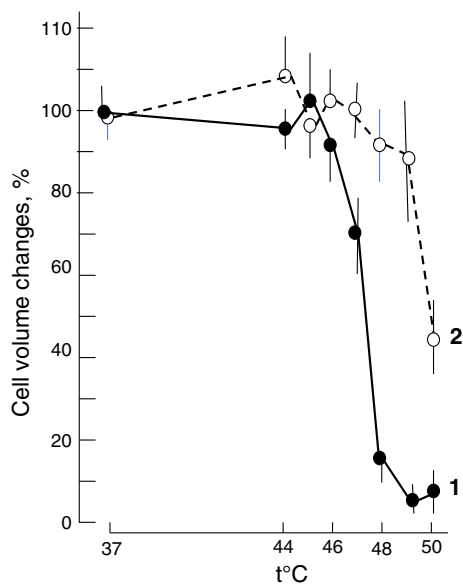

Fig. 8 The maximal amplitude of hyposmotic swelling (*curve 1*) and hyperosmotic shrinkage (*curve 2*) of A549 cells preincubated at the indicated temperatures for 10 min and then subjected to hyposmotic shrinkage and hyperosmotic swelling at 37 °C, as shown in Figs. 1 and 3, respectively. Mean $\pm$ SE from 5 independent experiments are reported. The maximal amplitude of cell shrinkage and swelling in cells preincubated at 37 °C was taken as 100 %

Fig. 9 Dependence of the ^{86}Rb influx rate mediated by Na^+, K^+, $2Cl^-$ cotransport (*curve 1*), and K^+ channels (*curve 2*) on incubation medium osmolality. Na^+, K^+, $2Cl^-$ cotransport was measured as the ouabain-resistant, bumetanide-sensitive component of the ^{86}Rb influx rate. K^+ channels were estimated as (ouabain + bumetanide)-resistant, Ba^{2+}-sensitive ^{86}Rb influx. Mean $\pm$ SE from experiments performed in quadruplicate are reported

called biogel) behaves as osmosensor (Fels et al. 2009). Data obtained in this study showed that the osmosensing properties of biogel play a key part in RVD evoked by exposure of A549 cells to hypotonic medium. This conclusion is supported by two major observations.
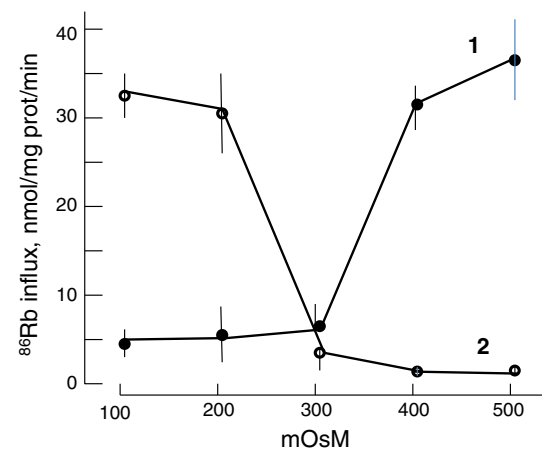
First, pretreatment of A549 cells at 48 °C sharply suppressed swelling triggered by hyposmotic medium (Figs. 3, 4, parameter $V_{max} - V_1$) as well as by their transfer from hypertonic to isosmotic solution (Figs. 1, 2, parameter $V_3 - V_2$). The inhibitory action of temperature elevation was also found in the study of isosmotic swelling evoked by dissipation of the transmembrane gradient of monovalent cations in ILS as well as by hyposmotic swelling of

Fig. 10 Effect of preincubation medium temperature elevation on baseline activity (curves 1) of K^+ channels (a) and Na^+, K^+, $2Cl^-$ cotransport (b) and their increments triggered by hyposmotic swelling and hyperosmotic shrinkage, respectively (curves 2). A549 cells were preincubated at the indicated temperatures for 10 min and then subjected to ion flux measurements in control and anisosmotic media at 37 °C. Mean ± SE from experiments performed in quadruplicate are reported
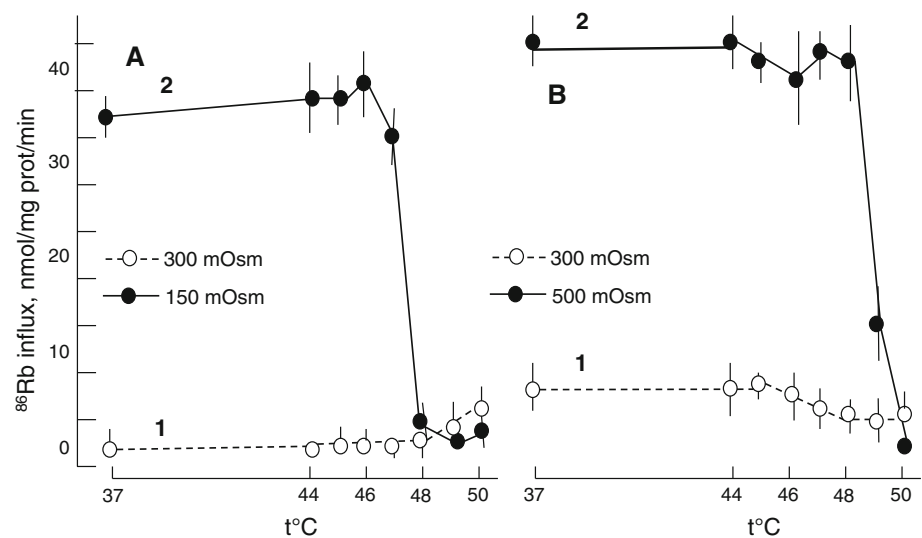
A549 cells with permeabilized plasma membrane (Fig. 5). Significantly, blockade of cell volume changes, triggered by hyposmotic medium, occurred with temperature elevation from 46 to 48 °C (Fig. 8). This observation is consistent with numerous reports demonstrating the narrow range of temperature increment that leads to gel-sol transition in different colloidal systems, including hydrogels (Harrison et al. 1971; Hench and West 1990; Chen et al. 2013). Viewed collectively, these results show that temperature elevation suppresses the osmosensing properties of A549 cells via its action on biogel rather than on plasma membrane permeability to water.

Second, side-by-side with blockade of cell volume changes in hyposmotic medium, 10-min preincubation at 48 °C completely abolished RVD as well as the increment of Ba^{2+}-sensitive K^+-channel activity (Fig. 10a), providing RVD in a large number of cells studied so far (Lang et al. 1998; Hoffmann et al. 2009).

In contrast to swelling, cell shrinkage in hyperosmotic medium was not affected by 10-min preincubation at 48 °C (Fig. 1). Additional experiments demonstrated that the maximal amplitude of hyperosmotic shrinkage decreased by twofold with preincubation temperature elevation to 50 °C (Fig. 8). We also discerned that identical treatment completely abolished the increment of Na^+, K^+, $2Cl^-$ cotransport activity seen in shrunken A549 cells (Fig. 10b). The former phenomenon is consistent with data on thermal inactivation of shrinkage-dependent Na^+, K^+, $2Cl^-$ cotransport in rat erythrocytes that correlate with spectrin annealing and disruption of the cortical cytoskeleton (membrane carcass) (Orlov et al. 1993; Parshina et al. 2013). Mechanisms underlying a distinct impact of temperature elevation on cell volume changes triggered by

biogel osmosensing properties in hypo- and hyperosmotic media remain unknown.

In conclusion, our results reveal that thermal inactivation of cytoplasmic gel swelling in hyposmotic medium is accompanied by inhibition of swelling-induced K^+ fluxes and RVD. The role of cytoplasmic gel osmosensitivity in intracellular signaling triggered by hyperosmotic shrinkage should be examined further.

References

Akimova OA, Bagrov AY, Lopina OD, Kamernitsky AV, Tremblay J, Hamet P, Orlov SN (2005) Cardiotonic steroids differentially affect intracellular Na^+ and $[Na^+]i/[K^+]i$-independent signaling in C7-MDCK cells. J Biol Chem 280:832–839

Boudreault F, Grygorczyk R (2004) Evaluation of rapid volume changes of substrate-adherent cells by conventional microscopy 3D imaging. J Microscopy 215:302–312

Brown A, Lasek RJ (1993) Neurofilaments move apart freely when released from the circumferential constrain of the axonal plasma membrane. Cell Motil Cytoskelet 26:313–324

Chen YY, Wu HC, Sun JS, Dong GS, Wang TW (2013) Injectable and thermoresponsive self-assembled nanocompositive hydrogel for long-term anticancer drug delivery. Langmuir 29:3721–3729

Colclasure GC, Parker JC (1992) Cytosolic protein concentration is the primary volume signal for swelling-induced K, Cl cotransport in dog red cells. J Gen Physiol 100:1–10

Di Ciano-Oliveira C, Thirone ACP, Szaszi K, Kapus A (2006) Osmotic stress and the cytoskeleton: the R(h)ole of Rho GTPases. Acta Physiol 187:257–272

Downey GP, Grinstein S, Sue-A-Quan A, Czaban B, Chan CK (1995) Volume regulation in leukocytes: requirement for an intact cytoskeleton. J Cell Physiol 163:96–104

Fels J, Orlov SN, Grygorczyk R (2009) The hydrogel nature of mammalian cytoplasm contributes to osmosensing and extracellular pH sensing. Biophys J 96:4276–4285

Fulton AB (1982) How crowded is cytoplasm. Cell 30:345–347

Gagnon F, Dulin NO, Tremblay J, Hamet P, Orlov SN (1999) ATP-induced inhibition of Na+, K+, Cl− cotransport in Madin–Darby canine kidney cells: lack of involvement of known purinoceptor-coupled signaling pathways. J Membr Biol 167:193–204

Groulx N, Boudreault F, Orlov SN, Grygorczyk R (2006) Membrane reserves and hypotonic cell swelling. J Membr Biol 214:43–56

Hallows KR, Packman CH, Knauf PA (1991) Acute cell volume changes in anisotonic media affect F-actin content of HL-60 cells. Am J Physiol 261:C1154–C1161

Hallows KR, Law FY, Packman CH, Knauf PA (1996) Changes in cytoskeletal actin content, F-actin distribution, and surface morphology during Hl-60 cell volume regulation. J Cell Physiol 167:60–71

Harrison MA, Morgan PH, Park GS (1971) A simple method for determining sol–gel transition temperatures in weak polymer jellies. Br Polym J 3:154–155

Hench LL, West JK (1990) The sol–gel process. Chem Rev 90:33–72

Hoffmann EK, Simonsen LO (1989) Membrane mechanisms in volume and pH regulation in vertebrate cells. Physiol Rev 69:315–382

Hoffmann EK, Lambert IH, Pedersen SF (2009) Physiology of cell volume regulation in vertebrates. Physiol Rev 89:193–277

Jakab M, Furst J, Gschwentner M, Botta M, Garavaglia ML, Bazzini C, Rodighiero S, Meyer G, Eichmuller S, Woll E, Chwatal S, Ritter M, Paulmichl M (2002) Mechanisms sensing and modulating signals arising from cell swelling. Cell Physiol Biochem 12:235–258

Kerrigan MJ, Hook CS, Qusous A, Hall AC (2006) Regulatory volume increase (RVI) by in situ and isolated bovine articular chondrocytes. J Cell Physiol 209:481–492

Koltsova SV, Platonova A, Maksimov GV, Mongin AA, Grygorczyk R, Orlov SN (2011) Activtion of P2Y receptors causes strong and persistant shrinkage of C11-MDCK renal epithelial cells. Am J Physiol Cell Physiol 301:C403–C412

Kuang K, Yiming M, Zhu Z, Iserovich P, Diecke FP, Fischbarg J (2006) Lack of threshold for anisotonic volume regulation. J Membr Biol 211:27–33

Lang F, Busch G, Ritter M, Volkl H, Waldegger S, Gulbins E, Haussinger D (1998) Functional significance of cell volume regulatory mechanisms. Physiol Rev 78:247–306

Luby-Phelps K (2000) Cytoarchitecture and physical properties of cytoplasm: volume, viscosity, diffusion, intracellular surface area. Int Rev Cytol 192:189–221

Martinac B (2011) Bacterial mechanosensitive channels as a paradigm for mechanosensory transduction. Cell Physiol Biochem 28:1051–1060

Minton AP (1981) Excluded volume as determinant of macromolecular structure and reactivity. Biopolymers 20:2093–2120

Minton AP, Colclasure GC, Parker JC (1992) Model for the role of macromolecular crowding in regulation of cellular volume. Proc Natl Acad Sci USA 89:10504–10506

Mongin AA, Orlov SN (2001) Mechanisms of cell volume regulation and possible nature of the cell volume sensor. Pathophysiology 8:77–88

O'Neil RG, Heller S (2005) The mechanosensitive nature of TRPV channels. Pfluger Arch—Eur J Physiol 451:193–203

O'Neill WC (1999) Physiological significance of volume-regulated transporters. Am J Physiol 276:C995–C1011

Orlov SN, Kolosova IA, Cragoe EJ, Gurlo TG, Mongin AA, Aksentsev SL, Konev SV (1993) Kinetics and peculiarities of thermal inactivation of volume-dependent Na/H exchange, Na, K, 2Cl cotransport and K, Cl cotransport in rat erythrocytes. Biochim Biophys Acta 1151:186–192

Orlov SN, Tremblay J, Hamet P (1996) Cell volume in vascular smooth muscle is regulated by bumetanide-sensitive ion transport. Am J Physiol 270:C1388–C1397

Orlov SN, Platonova AA, Hamet P, Grygorczyk R (2013) Cell volume and monovalent ion transporters: their role in the triggering and progression of the cell death machinery. Am J Physiol Cell Physiol 305:C361–C372

Papakonstanti EA, Vardaki EA, Stounaras C (2000) Actin cytoskeleton: a signaling sensor in cell volume regulation. Cell Physiol Biochem 10:257–264

Parker JC (1993) In defense of cell volume? Am J Physiol 265:C1191–C1200

Parshina EY, Yusipovich AI, Platonova AA, Grygorczyk R, Maksimov GV, Orlov SN (2013) Thermal inactivation of volume-sensitive K+, Cl− cotransport and plasma membrane relief changes in human erythrocytes. Pfluger Arch—Eur J Physiol 465:977–983

Pedersen SF, Nilius B (2007) Transient receptor potential channels in mechanosensing and cell volume regulation. Methods Enzymol 428:183–207

Platonova AA, Orlov SN, Grygorczyk R (2013) Volume changes triggered by aniosmotic media in intact and permeabilized cells: role of cytoskeleton network. Bull Siberian Med 12:60

Sachs JR (1998) How do red blood cells know how big they are? In: Okada Y (ed) Cell volume regulation: the molecular mechanism and volume sensing machinery. Elsevier Science, Tokyo, pp 3–13

Summers JC, Trais L, Lajvardi R, Hergan D, Buechler R, Chang H, Pena-Rasgado C, Rasgado-Flores H (1997) Role of concentration and size of intracellular macromolecules in cell volume regulation. Am J Physiol 273:C360–C370

Tatur S, Groulx N, Orlov SN, Grygorczyk R (2007) Ca2+-dependent ATP release from A549 cells involves synergic autocrine stimulation by coreleased uridine nucleotides. J Physiol 584:419–435